On The Role Of Soft Inclusions On The Fracture Behaviour Of Cement Paste

Mercuri, L.; Romero Rodriguez, Claudja; Xu, Yading; Chaves Figueiredo, Stefan; Mors, Renee; Rossi, Emanuele; Anglani, G.; Antonaci, P.; Šavija, Branko; Schlangen, E.

DOI
10.21012/FC10.235271

Publication date
2019

Document Version
Final published version

Published in
Proceedings of the 10th International Conference on Fracture Mechanics of Concrete and Concrete Structures

10^{th} International Conference on Fracture Mechanics of Concrete and Concrete Structures
FraMCoS-X
G. Pijaudier-Cabot, P. Grassl and C. La Borderie (Eds)
https://doi.org/10.21012/FC10.235271

ON THE ROLE OF SOFT INCLUSIONS ON THE FRACTURE BEHAVIOUR OF CEMENT PASTE

L. MERCURI[+], C. ROMERO RODRIGUEZ[†], Y. XU[†], S. CHAVES FIGUEIREDO[†], R. MORS[†], E. ROSSI[†], G. ANGLANI[+], P. ANTONACI[+], B. ŠAVIJA[†] AND E. SCHLANGEN[†,*]

[+]Politecnico di Torino
Turin, Italy
e-mail: s233035@studenti.polito.it; giovanni.anglani@polito.it; paola.antonaci@polito.it

[†]Delft University of Technology
Delft, Netherlands
e-mail: c.romerorodriguez@tudelft.nl; Y.Xu-5@tudelft.nl@tudelft.nl; s.chavesfigueiredo@tudelft.nl; R.M.Mors@tudelft.nl; e.rossi@tudelft.nl; b.savija@tudelft.nl; e.schlangen@tudelft.nl

Key words: Cement Paste, Work of Fracture, Tensile Strength, Durability

Abstract. Soft inclusions, such as capsules and other particulate admixtures are increasingly being used in cementitious materials for functional purposes (i.e. self-healing and self-sensing of concrete). Yet, their influence on the fracture behaviour of the material is sometimes overlooked and requires in-depth study for the optimization of mechanical and/or smart properties. An experimental investigation is presented herein on the role of bacteria-based lactate-derived particles on the fracture behaviour of cement paste in tensile configuration. These admixtures are currently used for the purpose of self-healing. Digital Image Correlation was used to obtain strain contours on the surface of the samples during the test. The influence of soft particles addition and age of the samples on the fracture mechanics of the composite were investigated.

1 INTRODUCTION

Micro and macro-cracks develop usually in concrete structures allowing corrosive agents to penetrate and consequently reduce the overall durability [1].

The process of deterioration in cementitious materials is accelerated when the exposed surface increases, therefore cracks are a severe threat to the safety and durability of concrete structures [2–6].

Self healing technology seems to be a good strategy to mitigate the direct and indirect costs related to repair of cracked concrete elements [7, 8]. Many types of self healing (SH) technology have been investigated in the past 20 years [9, 10] and capsules in particular demonstrated to be an efficient way to face the issue of protecting the healing agent prior to cracking while at the same time allowing the trigering of the healing mechanisms [3, 7, 9, 11, 12]. Despite the great interest shown on this technology, there are still relatively few studies concerning the effects that these particles have on the mechanical properties of the cementitious composites.

This study focuses on the role of soft inclusions on the mechanical behavior of notched cement paste samples with healing agent (HA) particles during Uniaxial Tensile Test (UTT). Three different particle types were investigated with respect to their bond strength with cement paste and the most promising type was chosen for the subsequent experiments. Then influence of soft particles and hydration degree of the compos-

ites were investigated through the analysis of measured properties such as stiffness, tensile strength and work of fracture.

2 MATERIALS AND TEST METHODS

2.1 Materials

Cement pastes were prepared by mixing ordinary Portland cement (OPC) CEM I 52.5 R with tap water with water-to-cement ratio (w/c) of 0.45, compliant with European standard EN-197-1 [13]. The healing agent (HA) particles were added to the paste specimens in dosage of 1.3% by weight of cement, which resulted in 1.5 % by volume of composite. The particles (maximum diameter of 3 mm) were composed of lactate bio-polymer, a calcium source and bacterial spores (of Bacillus cohnii-related strains). The activation nutrients were obtained from Corbion (Gorinchem, The Netherlands) [14]. Three polymer types were initally investigated, named P1, P2 and P3. Raw materials for their production were the same according to the supplier but each polymer underwent different production process resulting in different levels of chemical and physical interaction in the alkaline environment of the cement paste.

2.2 Sample preparation for bond strength test

For the investigation of the particle-cement paste bond strength bi-material samples were prepared consisting of equal parts of bio-polymer and cement paste. The whole sample dimension was 15 $mm \times 15\ mm \times 10\ mm$.

For the preparation of the polymeric part, previously crushed HA particles were placed inside a shallow circular mould and heated to the corresponding transition temperature (T_G). The T_G was different for each polymer and was determined as the temperature at which the polymer became homogeneous and could flow filling the free spaces among particles without suffering thermal degradation. When the heating temperature was too low only the surface particles melted whereas internally only the grain limbs melted. On the other hand when the heating temperature was too high air bubbles formed and parts of the polymer presented darkened areas. To prevent air bubbles and too high transition temperatures a constant pressure of 15.4 kPa was applied. Table 1 shows the temperatures at which each studied polymer was heated. After cooling, the polymer regained its original rigidity and was ready to be cut.

Table 1: Transition temperatures

P1	P2	P3
175 $\pm$ 5 °C	165 $\pm$ 5 °C	145 $\pm$ 5 °C

For each polymer, 5 samples were prepared as follows. The polymeric half was placed into the mould and the same volume of cement paste was poured to fill the other half. The samples were left for 24 h at laboratory conditions and then demoulded. After demoulding only samples that were not debonded were half wrapped (on the polymer side) and cured in a chamber at 20°C and 95% of relative humidity until the age of 28 days. In Figure 1 the resulting bi-material samples are shown. P3-cement paste debonded after demoulding and therefore the bond strength was considered nil.

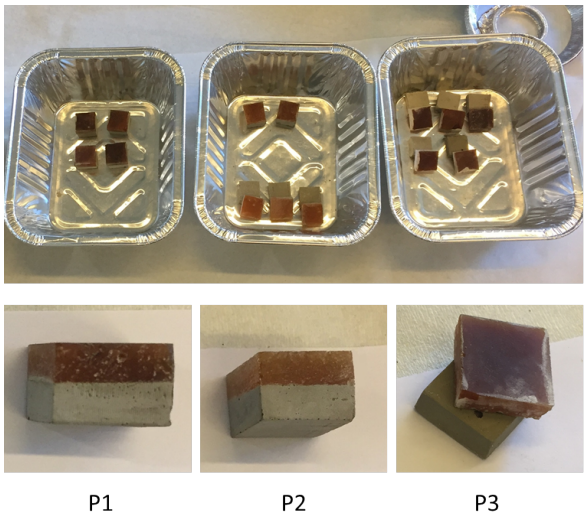

Figure 1: Demoulded bi-material samples prepared with P1, P2 and P3.

2.3 Sample preparation for UTT

For the UTT, cement pastes with and without HA particles (1.5 % by volume of composite) were cast into prismatic moulds with dimensions of 15 $mm\times$ 15 $mm\times$ 90 mm. A vibration plate was used to minimize entrapped air in the fresh cement paste. The samples were sealed and left at laboratory conditions for 24 h, then demoulded and cured in a curing chamber as described before.
After 7, 14 and 28 days, the samples were cut with a diamond saw into 15 mm side cubes and two notches of the same depth were made on two opposite sides of the cubes. The total length of the two notches was such that the area of the ligament was half of that of the un-notched section.

2.4 Bond strength test of bi-material prisms

For the measurement of the bond strength on bi-material samples uniaxial tensile test was carried out in a mini tension-compression stage with load cell of 500 N (Figure 4). The samples were glued to the loading plates which were connected to the frame through hinges, therefore allowing bending stresses. The test was performed in displacement control at a rate of 0.5 $\mu m/sec$. The bond strength was calculated from the measured peak load.

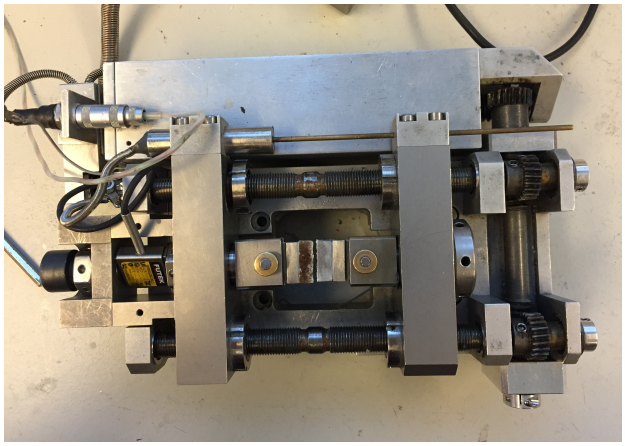

Figure 2: Mini TSTM tensile test setup after a test

2.5 Uniaxial Tensile Test of notched prisms

The UTT was performed by means of a servo hydraulic press Axial Tension-Compression Systems, model 8872 from Instron (High Wycombe, UK) on 6 samples per batch. The average vertical displacement of 2 Linear Variable Differential Transformers (LVDT) was used to control the test at a rate of 15 nm/s. The LVDT were positioned on opposite sides of the loading platens, coincident with the notched faces of the sample. In the configuration used the loading platens had high rotational stiffness with respect to the bending stiffness of the specimen, therefore they don't allow rotation of the faces of the sample where the tension is applied [15, 16]. Prior to the test the samples were glued to the loading platens in load control to prevent precracking due to the shrinkage of the pleximon glue. In Figure 2 the configuration described above is shown.

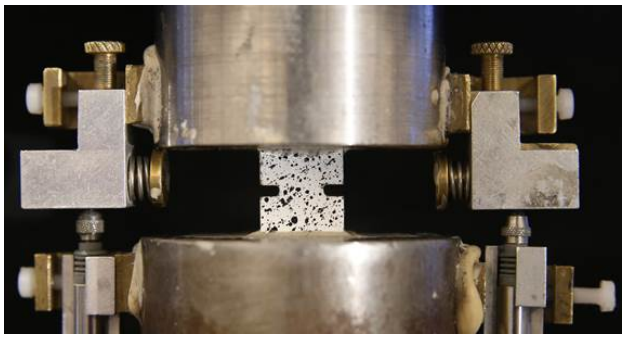

Figure 3: UTT configuration on a notched sample. The sample is tested with a dotted surface for DIC analysis.

From the obtained curves of Load vs. displacement it was possible to quantify the influence of inclusions on representative properties such as stiffness (K_t to have information during the elastic phase), tensile strength (f_t peak information) and work of fracture (W_f post peak behaviour). Moreover the curve behavior could provide qualitative information on the brittleness and complexity of the rupture mechanism. The work generated during the tensile test to completely fracture the sample was calculated as in [17]:

$$W_f = \int_{u_p}^{u_f} F \, \mathrm{d}u. \quad (1)$$

Where u_p corresponds to the elongation at the peak load and u_f to the final elongation. With regards to the elastic stiffness of the element, K_t, it was calculated simply as the quotient of the peak load and the deformation at the peak.

2.6 Digital Image Correlation (DIC) analysis

For each tensile test Digital Image Correlation (DIC) analysis was performed in order to track the sample surface displacements and to capture the crack pattern and crack nucleation. Freeware Ncorr [18] was used to perform the analysis.
Prior to UTT a thin layer of white paint was applied on one side of the sample and random black dots were marked in order to perform the analysis. The digital images were acquired at 1 frame per second during the test. The digital camera used was a *Canon EOS 6D*, with a resolution of 20.2 megapixel and a *MP-E 65mm f/2.8 1-5x Macro Photo* lens.

3 RESULTS AND DISCUSSION

3.1 Bond strength of polymer-matrix interface

All the tested samples failed near the interface particle-cement paste. In [Figure 4] the typical failure surfaces of the the bi-material samples are shown.

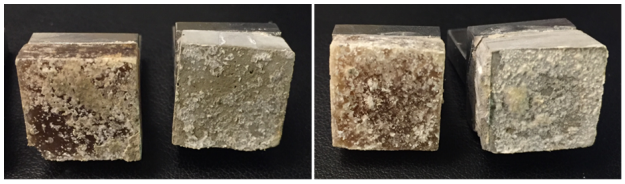

Figure 4: Effect of the chemical interaction on the ITZ between P1/P2 (left/right) and the cement matrix.

For both P1 and P2 a white precipitate was observed within the polymer-cement paste interface. It is believed from visualization of the interface that the bio-polymer was not inert in the alkaline environment of the cement paste and that calcium leachates from the bio-polymer are responsible for the observed precipitate [19]. Both the failure surfaces of the bi-material samples prepared from P2 show regular presence of the white precipitate, suggesting that the failure may have occurred within the layer of precipitate. Whereas when observing the fracture surfaces of P1 samples it is possible to observe that failure occurred both within the white precipitate and at the interface precipitate/polymer-cement paste surface. From the visual inspection there seems to be less white precipitate in P1 samples compared to P2.

In [Figure 5] the calculated bond strength from the uniaxial tensile test of bi-material samples are shown.

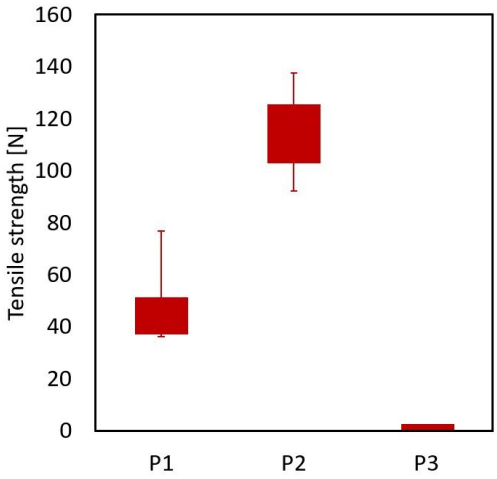

Figure 5: Tensile test results of the interface bond strength

The results show markedly higher bond strength of cement paste with polymer P2 when compared to P1. The stronger interface for P2 samples seems to be correlated to the higher amount of precipitate present at the interface. P2 was then used for the rest of the experiments. Note, again, that in P3 specimens the polymer had debonded from the cementitious matrix upon demoulding. Its bond strength is therefore taken as zero.

3.2 Uniaxial tensile test

In Figure 7 and 6 a typical DIC analysis of the sample surface and corresponding curve Load vs. vertical displacement, respectively, are shown.

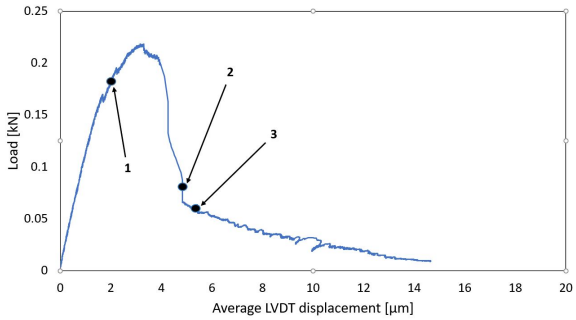

Figure 6: Typical load-vertical displacement for the used configuration and tested samples.

The specific test configuration of fixed platens and two-notched cubes resulted in a characteristic state of stresses arising in the sample as described in [15, 16, 20]. For the majority of the tested samples, under these conditions, a crack nucleated from one of the notches first, as visible in Figure 7 a) and then continued to propagate to the other notch until a certain moment, as in Figure 7 a). At this point the propagation of the first crack stopped and a new one nucleated from the opposite notch. As the first crack propagated and the ligament area was decreased, a bending moment arised due to the rotation restraint imposed by the rotationally-fixed loading platens until the tensile stresses at the opposite notch overcame locally the tensile strength of the material. Theoretically, this behavior can be noticed in plate-like specimens from the resulting load-displacement curves, where a plateau is observed between a certain stage during the propagation of the first crack and the nucleation of the second crack [21]. In most of the tested samples this "bump" or "waggling" was not evident from the obtained curves. In [15] the author explained that cubical shapes of the sample resulted in a triaxial stress state, in the sense that local rotations may arise along the diagonal not aligned with the LVDT and go undetected.

3.2.1 Influence of hydration age on the mechanical properties

In Figure 8 the calculated K_t, f_t and W_f are summarized for plain cement paste (CP) and for paste containing 1.3 $\%$ by weight of cement of polymeric particles (P2 1.3). These were assumed to come from normal distributions and were tested through one-sided Grubbs outlier tests. [22]

As an indication of the elastic properties of the studied composites the stiffness calculated from the elastic branch of the curves load-displacement was used [Figure 8 a)]. The stiffness of cement paste sample remains more or less constant with hydration time. The cement type used in the samples was CEM I 52.5R which hydrates faster than normal cement because of the higher specific surface. Nevertheless for samples containing SH capsules this was not the case.

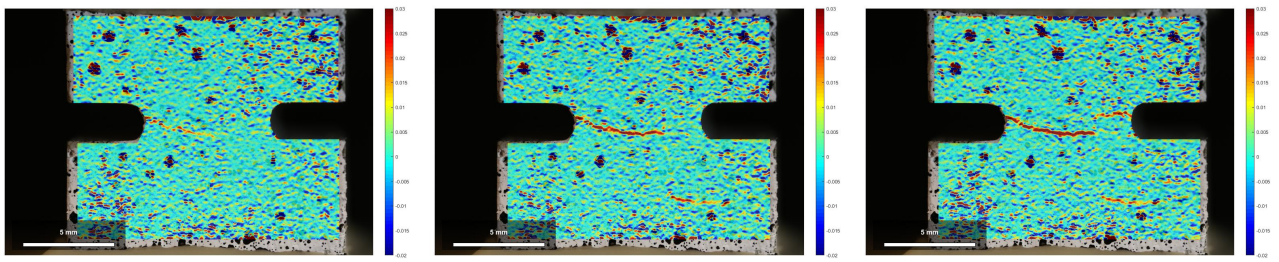

Figure 7: From left to right: first crack nucleation from the left notch after the peak load (corresponding to arrow 1 in Figure 6), first crack stopped (arrow 2), second crack nucleation from the right notch (arrow 3).

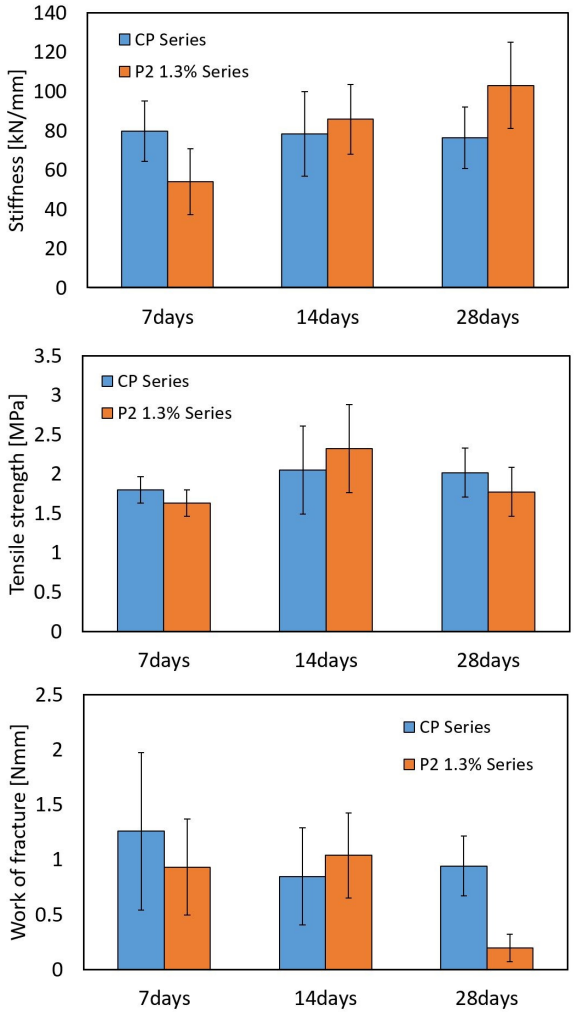

Figure 8: Stiffness, tensile strength and work of fracture of cement paste and P2 1.3 at ages 7, 14 and 28 days.

A clear increasing trend is noticeable and at 28 days the samples with HA particles present higher stiffness than the reference cement paste. The presence of the particles, which were proven to be reactive in the alkaline environment of cement paste, as shown in Section 3.1, seem to have modified the hydration of an influence zone around the particle.

Regarding tensile strength the cement paste samples show only small increases with increasing age [Figure 8. This mild strength development after 14 days is linked to the fast hydration of CEM I 52.5R, as discussed for the stiffness. In the case of P2 1.3 the trend of tensile strength development with age results somehow unclear. Overall, the strength increased mildly from 7 to 28 days (about 8 %), but an unexpected value of tensile strength was measured for 14 days, higher that that at 28 days. At 28 days of hydration the tensile strength of M1.3 was lower than that of CP around 3 % which overall can be translated as the particles having small impact on this property for the studied dosage.

Post peak behaviour of young samples both from CP and P2 1.3 presented high variability as evinced from the values of the work of fracture reported in [Figure 8 c)]. The evolution of the work of fracture for CP series is as reported for its other properties: no differences on the property value is noticeable from 14 to 28 days of hydration. On the other hand for P2 1.3 a slow development is still evident in the same interval of time with significantly decreased work of fracture of about 79 %. Pressumably the lactate particles influence the kinetics of cement hydration and/or interacts chemically with the cement in such a way that the achievement of the ”final” value of the property is delayed. Overall, cement paste samples presented significantly higher work of fracture than the paste with 1.3 % of inclusions.

4 CONCLUSIONS

Some conclusions can be derived from the work presented in this study regarding the influence of lactate-derived self-healing particles on the fracture behavior of cement paste:

- The lactate-derived HA particles P1 and P2 show different levels of reactivity in the alkaline environment of cement paste, resulting in different bond strengths with cement paste. A failure within the layer of precipitates between polymer and cement paste seems to yield higher bond strength than a failure along the interface cement paste-polymer/precipitate.

- From the comparison between the development in time of stiffness, tensile strength and work of fracture of plain and self-healing cement pastes is suggested

that the HA particles influence the hydration kinetics of cement or interact chemically with the surrounding paste over time.

- At an age of 28 days the addition of HA particles resulted in an increase in stiffness of 42 %, negligible decrease in the tensile strength of 3 % and dramatically reduction of the work of fracture at around 79 %.

ACKNOWLEDGEMENTS

The second author acknowledges the financial support from the Construction Technology Research Program funded by the Ministry of Land, Infrastructure and Transport of the Korean Government under the grant 17SCIP-B103706-03. The authors would like to thank Basilisk for providing the particles.

REFERENCES

[1] Shamsad Ahmad. Reinforcement corrosion in concrete structures, its monitoring and service life prediction—-a review. *Cement and concrete composites*, 25(4-5):459–471, 2003.

[2] Seung Jun Kwon, Ung Jin Na, Sang Soon Park, and Sang Hwa Jung. Service life prediction of concrete wharves with early-aged crack: Probabilistic approach for chloride diffusion. *Structural Safety*, 31(1):75–83, 2009.

[3] Guohao Fang, Yuqing Liu, Shaofeng Qin, Weijian Ding, Jianchao Zhang, Shuxian Hong, Feng Xing, and Biqin Dong. Visualized tracing of crack self-healing features in cement/microcapsule system with x-ray microcomputed tomography. *Construction and Building Materials*, 179:336–347, 2018.

[4] Vincent Picandet. *Influence d'un endommagement mécanique sur la perméabilité et sur la diffusivité hydrique des bétons*. PhD thesis, Université de Nantes, 2001.

[5] Alireza Akhavan, Farshad Rajabipour, et al. Quantifying the effects of crack width, tortuosity, and roughness on water permeability of cracked mortars. *Cement and Concrete Research*, 42(2):313–320, 2012.

[6] Kejin Wang, Daniel C Jansen, Surendra P Shah, and Alan F Karr. Permeability study of cracked concrete. *Cement and concrete research*, 27(3):381–393, 1997.

[7] Kim Van Tittelboom, Nele De Belie, Denis Van Loo, and Patric Jacobs. Self-healing efficiency of cementitious materials containing tubular capsules filled with healing agent. *Cement and Concrete Composites*, 33(4):497–505, 2011.

[8] H. E. Klatter. Life-cycle cost approach to bridge management in the netherlands. In *Elementary particle theory*, pages 179–188. Transportation Research Board.

[9] Nele De Belie, Elke Gruyaert, Abir Al-Tabbaa, Paola Antonaci, Cornelia Baera, Diana Bajare, Aveline Darquennes, Robert Davies, Liberato Ferrara, Tony Jefferson, et al. A review of self-healing concrete for damage management of structures. *Advanced Materials Interfaces*, 5(17):1800074, 2018.

[10] Haoliang Huang, Guang Ye, Chunxiang Qian, and Erik Schlangen. Self-healing in cementitious materials: Materials, methods and service conditions. *Materials & Design*, 92:499–511, 2016.

[11] Mathias Maes, Kim Van Tittelboom, and Nele De Belie. The efficiency of self-healing cementitious materials by means of encapsulated polyurethane in chloride containing environments. *Construction and Building Materials*, 71:528–537, 2014.

[12] Kim Van Tittelboom, Eleni Tsangouri, Danny Van Hemelrijck, and Nele De Be-

lie. The efficiency of self-healing concrete using alternative manufacturing procedures and more realistic crack patterns. *Cement and concrete composites*, 57:142–152, 2015.

[13] BS/EN. 197-1: 2011. *Cement Part 1: Composition, specifications and conformity criteria for common cements.*, 2011.

[14] Renee Mors and Henk Jonkers. Effect on concrete surface water absorption upon addition of lactate derived agent. *Coatings*, 7(4):51, 2017.

[15] Jan GM van Mier. *Fracture of concrete under complex stress*. Faculty of Civil Engineering, Delft University of Technology, 1986.

[16] JGM Van Mier and MB Nooru-Mohamed. Fracture of concrete under tensile and shear-like loadings. *Fracture Toughness and Fracture Energy-Test Methods for Concrete and Rock.(eds. Mihashi, H., Takahashi, H. & Wittmann, FH), Balkema, Rotterdam*, pages 549–516, 1989.

[17] Zdenek P. Baant and Mohammad T. Kazemi. Size dependence of concrete fracture energy determined by rilem work-of-fracture method. *International Journal of Fracture*, 51(2):121–138, 1991.

[18] B. Adair Blaber, J. and A. Antoniou. Ncorr: open-source 2d digital image correlation matlab software. *Experimental Mechanics*, 55(6):1105–1122, 2015.

[19] NB Singh, S Prabha, and AK Singh. Effect of lactic acid on the hydration of portland cement. *Cement and concrete research*, 16(4):545–553, 1986.

[20] DA Hordijk. Local approach to fatigue of concrete, doctor dissertation. *Delft University of Technology*, 1991.

[21] Jan GM Van Mier. *Fracture processes of concrete*. CRC press, 2017.

[22] Frank E Grubbs. Procedures for detecting outlying observations in samples. *Technometrics*, 11(1):1–21, 1969.